Inorganica Chimica Acta, 161 (1989) 153–163

Spectrochemical and Electrochemical Studies of 21-Thiatetra(*p*-tolyl)porphyrin and Its Copper(II) Complexes

JERZY LISOWSKI, MARIA GRZESZCZUK and LECHOSŁAW LATOS-GRAŻYNSKI*

Institute of Chemistry, University of Wrocław, F. Joliot-Curie St. 14, 50 383 Wrocław (Poland)

(Received May 30, 1988)

Abstract

Electrochemistry, NMR, ESR and UV–Vis spectroscopy of 21-thiatetra(*p*-tolyl)porphyrin (STpTPH) and respective copper(II) (21-thiatetra(*p*-tolyl)porphyrin)X Cu(STpTP)X (X = Cl^-, Br^-, HCO_3^-, ClO_4^-, PPh_3) complexes have been investigated.

Monothiaporphyrin is an analogue of widely studied tetraphenylporphyrin, where one of the pyrrole rings has been replaced by a thiophene moiety. The impact of the replacement and the coordinating abilities of thiophene sulfur have been studied. STpTPH undergoes a two step proton addition in dichloromethane. Mono- and dication formations result in distorting the planar thiaporphyrin structure as confirmed by NMR and UV–Vis data. The electronic spectra of Cu(STpTP)X have a similar pattern to the monocation form but the pronounced dependence of the band positions on the ligand character has been established. An ESR spectrum pattern is typical for quasi-tetragonal Cu(II) systems. Parallel features show well resolved seven lines associated with coordination of three nearly equivalent nitrogens. The ESR parameters, particularly hyperfine coupling constant A, have been correlated with the geometry of Cu(II) porphyrins or porphyrin-like ligands. The influence of the axial ligand on the ESR parameters has also been discussed. Cyclic voltammetry studies show that Cu(STpTP)X exhibits a well defined Cu(II)/Cu(I) reduction ($E_{1/2}$ = -0.14 ± 0.03 V depending on the axial ligand), reported previously only for Cu(II) N-substituted porphyrins but not for Cu(II) porphyrins. The second reduction step results in demetalation. The physicochemcial properties of Cu(STpTP)X are considerably different from Cu(TTP) and closely resemble those of Cu(II) N-substituted porphyrin. Comparison between the electrochemical and spectroscopical properties has been discussed in terms of the general stability of a Cu(II)–axial ligand bond.

*Author to whom correspondence should be addressed.

Introduction

An attractive modification of the metallotetraphenylporphyrin molecule would be to change the immediate environment around the central atom, which, in this case, means a change in the properties of one from four usually equivalent equatorial nitrogen donors.

Representative examples of such systems recently studied include complexes of *N*-alkyl(aryl)porphyrins [1, 2], *N*-oxide of octaethylporphyrin [3] and the products of the insertion of carbene or nitrene into the metal ion–nitrogen bond [4, 5]. These new macrocycles drastically change the properties of the formed metalloporphyrins compared to their regular metalloporphyrin analogues.

Some of these studies are prompted by biochemical aspects such as the reaction of alkylating agents with heme proteins which leads to the formation of N-substituted porphyrins via the intermediate iron–porphyrin complexes [6, 7] modified on one of nitrogens. The *N*-oxide porphyrin complexes have been treated as alternative models for highly oxidized forms of heme proteins (particularly cytochrome P-450 and peroxidases) as intermediates in heme catabolism [8, 9]. Continuing our interest in the chemistry and spectroscopical properties of the porphyrin systems with strong asymmetry imposed by modification of a porphyrin core [10–13], we began to investigate the porphyrins where one of the pyrrole rings had been replaced by a thiophene moiety (structure **1**). Generally, the coordinating ability of thiophene is rather limited and this aspect adds additional interest to the presented subject. Grigg *et al.* have described thiaporphyrins related to ethioporphyrins [14]. Previous studies have also addressed the spectroscopic, structural and electrochemical properties of dithiaporphyrins [15–18]. However, the coordinating properties of thiaporphyrins have been treated rather marginally [14, 15].

In this report we concentrate our effort on monothia analogues of widely studied tetraphenylporphyrins ($TPPH_2$). The only example of monothia-

0020-1693/89/$3.50

porphyrin synthesis is the route proposed by Grigg *et al.* [14] who used the {3 + 1} cyclization. This approach was not found to be suitable for $TPPH_2$ derivatives. Therefore we worked out another synthetic scheme based upon the dithiatetraphenylporphyrin (S_2TPP) procedure [15]. 2,5-Bis(*p*-tolylhydroxymethyl)thiophene was used as the starting point of the regular $TpTPH_2$ condensation in dilute solution in the presence of pyrrole and benzaldehyde. The ring closure leads to the expected macrocycle **1**.

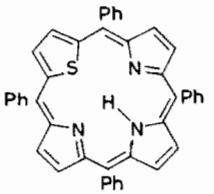

1

Recently we presented the results of an X-ray investigation of 21-thiatetra(*p*-tolyl)porphyrin (STpTPH) and copper(II) 21-thiatetra(*p*-tolyl)porphyrin bicarbonate ((CuSTpTP)HCO_3) [19]. Crystallographic studies of Cu(STpTP)HCO_3 demonstrated that Cu(II) possesses a five coordinate geometry. The thiophene sulfur forms a bond with Cu(II). The shape of the porphyrin resembles that seen in metal complexes of *N*-methylporphyrins [20].

Herein, we present the results of the systematic studies on properties of STpTPH and its copper complexes in solution. Particular emphasis is placed on electronic spectra, ESR and electrochemical investigation as a source of insight into the electronic structure and geometry of these low symmetry porphyrin-like species. The protonation mechanism of STpTPH followed by means of ^1H NMR has also been considered.

In addition, a comparison of Cu(II)tetraphenylthiaporphyrins with Cu(II)*N*-alkylporphyrins and Cu(II)tetraphenylporphyrin illuminates the effect of stereochemistry upon the redox potential, optical spectra and ESR parameters of these Cu(II) complexes which differ only in the character of an equatorial donor.

Experimental

Synthesis

21-Thiatetra(p-tolyl)porphyrin (STpTPH)

The condensation of 2,5-bis(*p*-tolylhydroxymethyl)thiophene (0.02 mol) with *p*-tolylaldehyde (0.04 mol) and pyrrole (0.06 mol) in boiling propionic acid (400 cm^3) conducted over 1 h, followed by cooling, produces a mixture from which STpTPH, $TpTPH_2$ and traces of S_2TpTP crystallize on standing for 24 h. The solid material was dissolved in carbon tetrachloride and subjected to chromatography on basic alumina with $CCl_4/CHCl_3$ (10:1 vol./vol.). Two major bands eluted to give $TpTPH_2$ and STpTPH successively. The fraction containing STpTPH was evaporated and the product recrystallized from dichloromethane/ethanol to give STpTPH in 5% yield.

For electronic spectra STpTPH samples were heated in a chloroform/benzene mixture in the presence of 2,3-dichloro-5,6-dicyanobenzoquinone under reflux for 0.5 h and purified chromatographically [21].

^{63}Copper(II)thiatetra(p-tolyl)porphyrin bicarbonate

A sample of Cu(STpTP)HCO_3 which was enriched in ^{63}Cu was prepared from ^{63}CuO (99.8%) which was converted into its chloride salt. A solution of $^{63}CuCl_2 \cdot 2H_2O$, 20 mg (0.12 mmol) in 2 ml of ethanol, was added to a solution of STpTPH (1.5 mg, 0.002 mmol) in 2 ml of chloroform in the presence of collidine (1 μl) and solid sodium carbonate. The solution was heated under reflux for 0.5 h and filtered to remove sodium carbonate. After evaporation of the solvent the residue was dissolved in dichloromethane and subjected to chromatography on neutral alumina and recrystallized from dichloromethane/hexane. All spectral parameters were similar to those described previously [19].

Copper(II)21-thiatetra(p-tolyl)porphyrin chloride

A solution of $CuCl_2 \cdot 2H_2O$ (50 mg, 0.3 mmol) in 10 ml of methanol was added to the solution of STpTPH (30 mg, 0.043 mmol) in 20 ml of chloroform and then mixed for 0.5 h. The reaction mixture was chromatographed on neutral Al_2O_3 to remove the traces of STpTPH and $STpTPH_2^+$. The column was eluated with $CHCl_3$ and in the following step with $CHCl_3/CH_3OH$ 10:1 vol./vol. The required compound was recovered from the second fraction after vacuum evaporation and recrystallization. Cu(STpTP)Br was synthesized in a similar manner starting from $CuBr_2$.

Solvents

1,2-Dichloroethane, methylene chloride and chloroform were routinely purified by washing with concentrated sulfuric acid, water, 1 M K_2CO_3, washing with water, drying over solid Na_2CO_3 and distilling. Chlorinated solvents were stored on 3 Å molecular sieves and protected from light. For the electrochemical studies 1,2-dichloroethane was additionally distilled from CaH_2 under nitrogen. Acetonitrile was refluxed and distilled over P_2O_5, distilled from CaH_2 and stored over molecular sieves. All other common solvents (THF, benzene, toluene, methanol) were thoroughly dried in the appropriate manner [22] and were distilled prior to use. Deuter-

ated solvents $CDCl_3$ (IBJ) and CD_2Cl_2 (Aldrich) were purified by passing through basic alumina and kept over molecular sieves in the dark.

Tetra(n-butyl)ammonium perchlorate (TBAP) was synthesized from TBAOH and $HClO_4$ and recrystallized from pentane/ethyl acetate mixture as previously described [23]. TBABr and TEACl were recrystallized from pentane/chloroform mixture.

Spectroscopic Instrumentation

Nuclear magnetic resonance spectra were recorded in the pulse FT mode on Tesla BS 567A and Jeol PS 100 spectrometers. Chemical shift was referenced to TMS. Electronic spectra were recorded on Cary 14 and Specord spectrometers. Electron spin resonance spectra were obtained with a JES-ME-3X X band spectrometer. Solutions of approximately 2 mM in $CHCl_3$/toluene (2:1) were examined.

Electrochemical Instrumentation and Procedures

Apparatus for cyclic voltammetry consisted of a Potentiostat type EP22 (Elpan) with IR compensation circuitry, Potentiostat-Generator type PG30/1 (ASP Lodz), Digital voltmeter type V540 (Meratronik) and XY recorders (type NE-240 EMG and SEFRAM). Cyclic voltammograms were recorded at potential scan rates from 20 to 500 mV/s. A typical three electrode cell was used for measurements with a Pt-disc working electrode (the geometric area = 0.01 cm^2), Pt-foil auxiliary electrode and commercial SCE(NaCl) as a reference electrode. The latter was separated from the working electrode compartment by a fritted glass bridge filled with the supporting electrolyte–solvent solution. The potential of this reference electrode in 0.1 M TBAP–$C_2H_4Cl_2$ is 0.64 V versus bis(biphenyl)chromium(I)/bis(biphenyl)chromium(0) reference redox system. All potentials reported in this work are expressed versus SCE and they are not corrected for liquid junction potentials. 1,2-Dichloroethane and acetonitrile were used as solvents in electrochemical measurements. Solutions of TBAP or TBABr (0.1 M) were supporting electrolytes. The concentration of electroactive species in the cell solution ranged from 10^{-4} M to 10^{-3} M. The cell was thermostated at 25.0 ± 0.5 °C and the cell solution was deoxygenated by a stream of purified nitrogen or argon presaturated with a solvent vapour. A blanket of the inert gas was maintained over the solution during voltammetric experiments.

Results and Discussion

Electronic Spectra

In Table 1 the optical spectra of 21-thiatetra(*p*-tolyl)porphyrin are presented. For comparison the spectra of $TPPH_2$ and S_2TPP are also included [15]. As is the custom with porphyrin spectra a distinction is made between the intensive Soret band in the near ultraviolet and four Q bands in the visible spectrum. Although we do not want to give a detailed interpretation some trends are discernible which can give information about the configuration of STpTPH in solution.

We can observe in Table 1 several effects due to the introduction of a sulfur atom. (a) The absorption frequency of the Soret band shows a bathochromic shift as compared to $TPPH_2$ itself. (b)

TABLE 1. Electronic spectra of thiaporphyrin (STpTPH) and its Cu(II) complexes[a] (S_2TPP and H_2TPP included for comparison)

Compound	Soret λ_{max} ($\epsilon \times 10^{-3}$)	Q bands λ_{max} ($\epsilon \times 10^{-3}$)			
H_2TPP[c]	419(464)	485(3.8) 515(18.7)	548(8.6)	592(5.5)	647(3.9)
STpTPH	428(380)	514(28)	550(11)	618(4.2)	680(4.9)
S_2TPP[c]	435(297.5)	515(29.6)	548(7.2)	635(2.2)	699(4.6)
$STpTPH_2^+$	440(266)		550(10)	610(16)	660(17)
$STpTPH_3^{2+}$	460(320)				710(46)
Cu(STpTP)Cl	475(96)		580(10.2)	635(8.3)	720(7.3)
Cu(STpTP)Br	470(80)		575(9.6)	630(8.6)	715(6.3)
$Cu(STpTP)PPh_3$	440(89) 460(85)		565(10.5)	625(7.8)	700(4.3)
$Cu(STpTP)HCO_3$	455(100)		565(10.9)	600(8)	695(4.3)
$Cu(STpTP)ClO_4$	445(114) 460(90)		560(13.4)	595(11)	690(3.5)
$Cu(STpTP)HCO_3$[b]	440(104) 465(78)		570(10.3)	610(7.7)	690(4.6)
Cu(STpTP)Cl[b]	440(104) 465(78)		570(10.3)	610(7.7)	690(4.6)

[a]If not stated differently measurements made in CH_2Cl_2. [b]In CH_3OH. [c]Ref. 15.

The introduction of sulfur causes a bathochromic shift of Q bands I and II while bands III and IV are much less effected. (c) For the Q band I the intensity is larger than for band II (reversed order as in the $TPPH_2$ case). The observed effects are more pronounced as the number of nitrogen atoms replaced is increased, i.e. in the series $TPPH_2 < STpTPH < S_2TPP$. It is clear that the number of heteroatoms has a significant and systematic effect on the energy levels in the macrocycles under discussion.

Spectroscopic titration of STpTPH with trifluoroacetic acid (TFA) in dichloromethane solution gave results analogous to those obtained for NCH_3-TPPH [24]. Both the green mono- and dications were obtained and well defined isosbestic points were observed (Fig. 1) for the separate processes of the proton addition. The conjugated acids of STpTPH show the considerable bathochromic shift of the Soret band. The number of separate Q bands decreases due to the protonation (Table 1). A similar titration in chloroform gave evidence only for the equilibrium between STpTPH and its dication. Supposedly the pK values in this system are too close to allow the distinction between $STpTPH_2^+$ and $STpTPH_3^{2+}$ spectroscopically. A similar conclusion was reached by ^1H NMR spectroscopy (*vide infra*).

Cu(STpTP)X complexes exhibit very similar spectra which are characterized by three prominent bands in the region 500–700 nm and a Soret band at about 440 nm. The spectrum pattern of the complexes closely resembles that recorded for the monocation $STTPH_2^+$ (Fig. 2). The number of bands and their positions are also similar to those encountered fro $Cu(NCH_3TPP)Cl$ but completely different from that found in the CuTPP case [25]. The noticeable influence of an axial ligand has been noticed. Because of that the metathesis of $Cu(STpTP)HCO_3$ could be followed by means of electronic spectroscopy. A weakly bonded HCO_3^- ligand has been easily exchanged in the presence of TBAX (X = ClO_4^-, Br^-, Cl^-) salts, added in excess, for the respective X anion. The replacement of HCO_3^- by neutral ligands e.g. PPh_3, CH_3OH, added in large excess, has also been demonstrated.

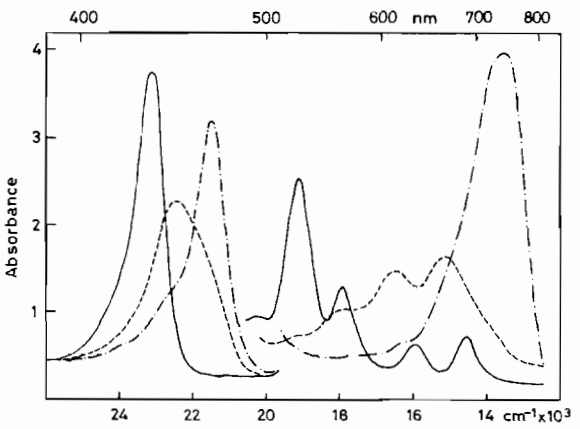

Fig. 1. Electronic spectra of dichloromethane solutions of: (a) STpTPH (——), (b) monocation $STpTPH_2^+$ (– – –), (c) dication $STpTPH_3^{2+}$ (– · –).

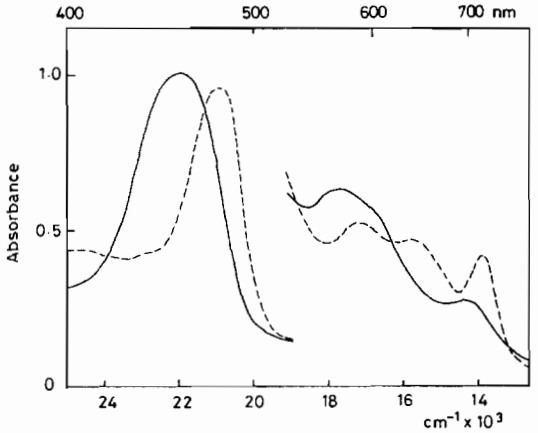

Fig. 2. Electronic spectra of dichloromethane solutions of: (a) $Cu(STpTP)HCO_3$ (——), (b) Cu(STpTP)Cl (– – –).

The spectra of the samples obtained via metathesis directly in a UV cell and those synthesized independently are identical. The bathochromic shift increases in the series ClO_4^-, HCO_3^-, PPh_3, Br^-, Cl^-.

The solvent effect has also been observed. In particular, the toluene solutions of Cu(STpTP)X present electronic spectra bathochromically shifted with respect to their dichloromethane counterparts.

A major feature to be considered in the interpretation of these spectra is the role of the phenyl rings at the *meso* positions. In solution when the ligand is not protonated (coordinated) the phenyl rings are constrained to be on average nearly perpendicular to the macrocycle system due to the proximity of the *ortho* hydrogen atoms of the phenyl ring and the β-hydrogen of the neighbouring pyrroles or thiophene rings [26]. The protonation (*vide infra*) and coordination of STpTPH must cause a distortion of the porphyrin system from planarity. The phenyl ring would have greater freedom to rotate allowing participation of the delocalized benzene electrons in the conjugated system of thiaporphyrin [27].

In our opinion, this mechanism accounts for the observed bathochromic shifts for the mono- and dication. Probably, the bathochromic series (see above) of Cu(STpTP)X reflects the changes in geometry due to the X ligand bonding properties. The relatively stronger ligands cause the more pronounced effect. The position of the monocation bands (Table 1) is consistent with the smaller distortion of the thiaporphyrin ring compared to the Cu(STpTP)X complexes. In the former one the thiophene ring should remain in the plane of pyrrole C (*vide infra*), in the latter the thiophene ring is markedly bent out of this plane [19].

TABLE 2. ^{1}H NMR parameters of thiaporphyrin (STpTPH) and its conjugated acids[a] ($TPPH_2$ and S_2TPP included for comparison)

	Thiophene A	Pyrrole C	Pyrrole B, D			*ortho*	*meta*	*p*-Methyl
			ν_1	ν_2	δ_{AB}			
STpTPH	9.81	9.00	8.72	8.64	7.6	8.14	7.63	2.82
$STpTPH_2^+$	9.81	8.95	8.92	8.78	13.2	8.28	7.75	2.77
$STpTPH_3^{2+}$	9.45	8.62	8.96	8.76	19.6	8.52	7.90	2.75
Δ_1	0.00	−0.05	0.20	0.14	5.6	0.14	0.12	−0.05
Δ_2	−0.36	−0.33	0.04	−0.02	6.4	0.24	0.15	−0.02
Δ_3	−0.36	−0.38	0.24	0.12	12.0	0.38	0.27	−0.07
$STpTPH_3^{2+}$ [b]	9.27	8.46	8.76	8.56	20.4	8.16	7.60	2.36
$TPPH_2$ [c]		8.72				8.30	7.80	
S_2TPP[c]	9.64	8.65				8.22	7.79	
Zn(STPP)Cl	9.45	8.80	8.95			8.15	7.80	

[a]If not stated differently measurements made in CD_2Cl_2. [b]In TFA. [c]Ref. 17. Chemical shifts given in ppm vs. TMS, δ_{AB} in Hz. Δ_i = increments of NMR parameters (i = 1, monocation vs. neutral form; i = 2, dication vs. monocation; i = 3, dication vs. neutral form) given in ppm.

Nuclear Magnetic Resonance Studies

The NMR parameters of STpTPH, and its mono- and dication forms are presented in Table 2. For comparison the respective data of $TPPH_2$ and S_2TPP have also been included.

The NMR spectroscopic titration was carried out by gradual addition of TFA to a solution of STpTPH in CD_2Cl_2 or $CDCl_3$. During the titration (25 °C) the average chemical shift was observed. The exchange of proton between ionic forms in the system is fast in the NMR time scale.

Two separate processes could be established in CD_2Cl_2 (Fig. 3) but only one in $CDCl_3$ (STpTPH $STpTPH_3^{2+}$) identically as for electronic spectroscopy.

In this paper we intend to discuss the results of the CD_2Cl_2 system. The formation of the mono- and dication strongly influences the chemical shifts but differently for each cation. This fact is illustrated by the increments of the chemical shifts produced by each protonation step (Table 2). For the 1:1.1 STpTPH:TFA molar ratio the monocation dominated the composition of the solution.

The corresponding shift values are treated as those reflecting monocation properties. The addition of the first proton results in the large increase of the chemical shift of the β-pyrrole protons of the B and D rings. The shifts of thiophene as well as the β-proton of the C ring are not changed. In the NMR spectrum of the dication the farther but small increase of the shifts for the β-protons of B and D rings has been noticed. On the other hand the protons of thiophene and C rings exhibit upfield shifts in the dication compared to both neutral and monocation forms. The resonances of the peripheral protons on the B and D rings form an AB quartet. The systematic increase of the shift difference between two coupled protons was observed as the number of

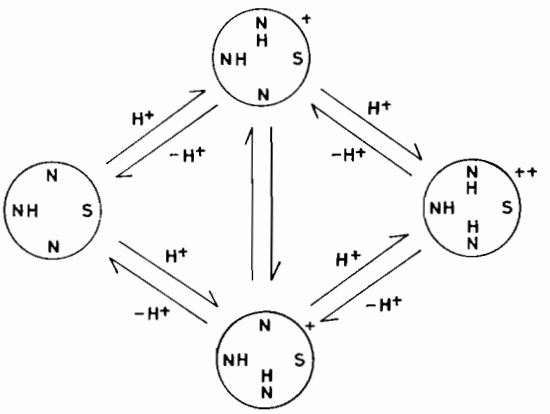

Fig. 3. Protonation scheme of STpTPH.

protons added was increased (Table 2). In order to understand these results we have to consider the following, competing effects.

(a) The introduction of positive charges into the thiaporphyrin molecule causes the downfield shift of the β-pyrrole proton resonances.

(b) Steric hindrance, that is, the effect that reduces the $\pi-\pi$ overlap by distorting the planar macrocycle structure causes a decrease in ring current (upfield shift).

(c) The nonplanarity of the conjugated acid leads to the release of the repulsive interaction between the *ortho* hydrogen of the phenyl ring and the β-hydrogen of the porphyrin allowing the phenyl ring to rotate toward the thiaporphyrin plane [27, 28]. These two structural effects (b and c) cause shielding on the β-protons of pyrroles and thiophene which results in the respective upfield shifts. The previously described experimental data of the protonation process can be accounted for by combination of all three mechanisms listed above. We par-

ticularly related them to the geometry rearrangements. We propose the protonation scheme given in Fig. 3. The location of the NH proton in the neutral form is well established and the long range coupling between the NH proton and the β-pyrrole proton of the C ring has been observed. The chemical shift confirms the pyrrolenine character of the ring under discussion. In the same way B and D rings are characterized by the shift of β-pyrrole protons of $TPPH_2$ (Table 2). All results are consistent with the proposed structure of STpTPH. The *trans* position with respect to thiophene sulfur allows for the nearly planar structure of the STpTPH molecule. The eventual tautomeric forms with the NH proton located in the closest neighborhood of sulfur (ring B or D) would make such a configuration less stable due to the NH–S steric interaction. Because of that, the formation of the monocation causes electrostatic repulsion as well as steric crowding in the porphyrin core. These are released by tilting of the pyrroles B or/and D out of the thiaporphyrin plane. The observed changes of chemical shifts reflect this rearrangement. The effect is restricted only to the ring undergoing protonation. Each monocation form is expected to present a NMR spectrum reflecting an intrinsic asymmetry of the ionic species, i.e. six pyrrole resonances. A fast NH proton exchange between two tautomeric forms (Fig. 3) has been invoked to explain the observed NMR pattern as the chemical shift averaging reduces the number of pyrrole resonances to those observed. The total effect can be explained by the action of mechanisms a and b discussed above. Further protonation (monocation transfer) would increase the steric interaction in the center of the macrocycle and force thiophene and all pyrrole rings out of plane which would account for the decrease of chemical shifts of the β-protons (mechanisms b and c).

Identical shift changes for both thiophene and pyrrole C, i.e. for rings which are not directly involved in protonation (see Fig. 3) confirm such a hypothesis. However one can see (Table 2) that the net effect in this protonation step is much smaller for the B and D pyrrole rings.

In this case the structural effects (b and c) are compensated for by addition of the second proton to rings B or D (mechanism a). The pronounced deviation from planarity is also reflected by the NMR spectrum of the phenyl rings. The splitting of the *ortho*-phenyl and *meta*-phenyl proton resonances (ABCD pattern) which are equivalent in the neutral form (AA'BB' pattern) has been observed for the monocation and dication. Such splitting is characteristic of porphyrin and metalloporphyrin where the mirror symmetry plane located in the plane of the porphyrin is removed [29].

The chemical shifts and spectrum pattern of the dication are similar to those recorded for Zn(STTP)Cl [30] (Table 2). The structure of Zn(STPP)Cl is not defined yet but one has to expect a large deviation from planarity as observed in $Cu(STpTP)HCO_3$. It is apparent that the same concept explains both dication and Zn(II) complex shifts.

In the NMR spectrum of the dication in TFA there are two NH resonances at −2.66 (B and D rings) and −2.97 (ring C) ppm. A variable temperature experiment with the dication in TFA showed that at about 50 °C the NH resonances disappeared. It is assumed that the NH protons undergo a rapid exchange with acid.

Electron Spin Resonance

Characteristic electron spin resonance spectra for samples containing 99.8%. ^{63}Cu are shown in Fig. 4.

The $^{63}Cu(STpTP)HCO_3$ spectrum shows well resolved copper parallel features, the two lowfield ones showing well resolved additional splitting into seven lines associated with interaction of the electron with three nearly equivalent nitrogen atoms. The copper perpendicular features are also split due to

TABLE 3. ESR parameters of copper(II) porphyrins

Complex	$g_{\parallel}$	$g_{\perp}$	$A_{\parallel}^{Cu}$	g_{iso}	A_{iso}^{Cu}	Reference
$Cu(STpTP)ClO_4$	2.171	2.050	185.5	2.094	88.0	this work
$Cu(STpTP)HCO_3$	2.192	2.063	169.7	2.117	69.5	this work
$Cu(STpTP)PPh_3$	2.189	2.056	166.5	2.108	63.5	this work
Cu(STpTP)Br	2.207	2.069	161.0	2.129	66.6	this work
Cu(STpTP)Cl	2.212	2.051	159.5	2.141	70.0	this work
CuTPP	2.190	2.045	211			33
$Cu(N\text{-}CH_3TPP)Cl$	2.256	2.080	172			10
Cu(NOOEP)	2.196		170	2.082	75.0	3
Cu(OEFB)	2.174	2.029	171.7	2.080	72.16	35
Cu(X-DPM)	2.224	2.039	154	2.113	55.6	34
	;	;	;	;	;	
	2.279	2.070	103	2.130	83.1	

Abbreviations: NOOEP, octaethylporphyrin *N*-oxide; OEFB, octaethylformylbiliverdin, X-DPM, substituted dipyrromethenes.

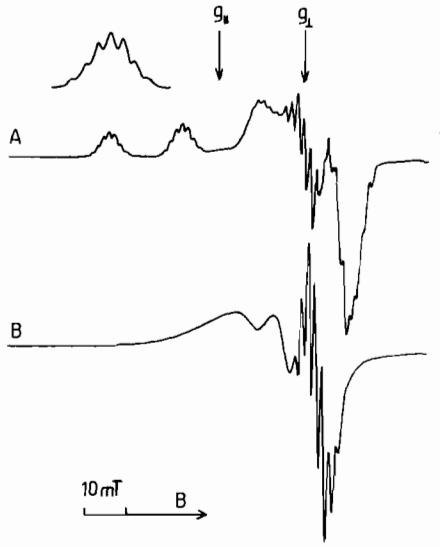

Fig. 4. ESR spectra of $^{63}Cu(STpTP)HCO_3$: A, frozen toluene:chloroform 1:2 vol./vol. solution, at 77 K; B, toluene: chloroform 1:2 vol./vol. solution, at 298 K.

the hyperfine (^{63}Cu) and superhyperfine (^{14}N) interactions and these are overlapped considerably. The 'anomalous' line is also observed. The spectrum pattern is typical for quasi-tetragonal copper(II) complexes [31] in spite of the porphyrin core modification and a considerable distortion from planarity [19]. These factors did not remove, however, the ESR equivalence of the N1, N2 and N3 atoms (A_{iso}^N = 14.8 $cm^{-1} \times 10^{-4}$, $A_\perp^N$ = 12.9 $cm^{-1} \times 10^{-4}$, $A_\parallel^N$ = 15.3 $cm^{-1} \times 10^{-4}$ for $Cu(STpTP)HCO_3$).

Consequently, the following discussion is going to be carried out in terms of quasi tetragonal symmetry (i.e. $g_1 \approx g_2 < g_3$). The relevant ESR parameters are presented in Table 3 for the series of Cu(STpTP)X complexes. The respective parameters for various Cu(II)–porphyrin derivatives are also included. The hyperfine coupling constant $A_\parallel^{Cu}$ decreases considerably in the series CuTPP [33], Cu(NCH_3TPP)Cl [10], Cu(NOOEP) [3], Cu(biliverdins) [34], Cu(dipyrromethanes) [35]. It reflects the deviation from the planar structure characteristic for CuTTP [32]. The direct mixing of 4s metal orbital to the ground state of Cu(II), caused by the symmetry lowering is responsible for the dependence discussed [10, 36]. However, the related changes in the character of the Cu(II)–porphyrin bond, i.e. decrease of covalency and π–π overlap, are also essential.

Applying known relations [33, 37] between the ESR parameters and molecular orbital coefficient [38] the following values have been calculated for $Cu(STpTP)HCO_3$: α^2 = 0.72 and α'^2 = 0.28. (The abbreviations and constant values as in ref. 38.) The covalency in $Cu(STpTP)HCO_3$ seems to be large but smaller than in the CuTPP or CuPc cases [38].

The ESR parameters are sensitive to the change of the axial ligand (Table 3). This observation has been used for analytical purposes to confirm the composition of the first coordination sphere in other experiments presented in this paper. Considerable differences (e.g. a difference 26 cm^{-1} of $A_\parallel^{Cu}$ comparing ClO_4^- (weakly bound) and Cl^- (strongly bound)) resulting from the character of the axial ligand suggest both the modification of geometric and electronic structures.

The modification of one from four equatorial TPP donors (N versus N–O, NCH_3 or S) has a strong influence on the ESR parameters. However, the parameters for the modified systems are noticeably close to each other, which is surprising considering the essentially different character of the fourth donor. It emphasizes the responsibility of the geometric factor for the ESR parameter values.

Electrochemical Studies

A cyclic voltammogram of STpTPH in 1,2-dichloroethane is shown in Fig. 5. One reduction and one oxidation process are observed. Their characteristics (i.e. anodic–cathodic peak separations, ratio of peak currents) indicate reversibility of heterogeneous electron transfer on the time scale of low potential scan measurements (20–300 mV s^{-1}). The observed electrode processes can be represented by reactions (1) and (2)

$$STpTPH + e \rightleftharpoons STpTPH^{-\cdot} \quad (1)$$
$$E = -1.065 \pm 0.005 \text{ V}$$

$$STpTPH - e \rightleftharpoons STpTPH^{+\cdot} \quad (2)$$
$$E = 1.035 \pm 0.005 \text{ V}$$

The respective cation and anion radicals are formed in the course of the redox processes. The oxidation and reduction potentials are shifted in a positive direction with heterosubstitution as compared to $TPPH_2$. The difference between the first oxidation potential and the first reduction potential (Δ) decreased referring to $TPPH_2$. Both electrochemical parameters fit quite well to reported dependencies of $E_{1/2}$ versus the chemical shift of β-hydrogen and (Δ) versus the energy of the Soret band reported by Ulman *et al.* for S_2TPP and analogues [18].

Cyclic voltammograms for the reduction and oxidation of Cu(STpTP)X (where X = axial ligand) show an apparent complexity of electrode processes (Fig. 5).

The following scheme can be used to describe the electrode processes and chemistry involved

Reduction

Wave 1:

$$Cu(II)(STpTP)X + e \rightleftharpoons [Cu(I)(STpTP)X]^- \quad (3)$$

Waves 2–3:

$$[Cu(I)(STpTP)X]^- + e \rightleftharpoons [Cu(STpTP)X]^{2-} \quad (4)$$

$$[Cu(STpTP)X]^{2-} \xrightarrow[-X^-]{+H^+} Cu + STpTPH \quad (5)$$

$$STpTPH + e \rightleftharpoons STpTPH^{\cdot} \quad (6)$$

Wave 4:

$$STpTPH^{\cdot} + e \rightleftharpoons STpTPH^{2-} \quad (7)$$

Oxidation

Wave 1:

$$Cu(II)(STpTP)X - e \rightleftharpoons [Cu(II)(STpTP)X]^{+\cdot} \quad (8)$$

Wave 2:

$$[Cu(II)(STpTP)X]^{+\cdot} - e \longrightarrow \text{products chemically irreversible} \quad (9)$$

Characteristic potentials for the electrode processes of $Cu(STpTP)HCO_3$ are collected in Table 4.

The most interesting feature present in the cyclic voltammogram of Cu(STpTP)X that is absent for STpTPH is the appearance of a wave at *c.* −0.1 V, i.e. in the range completely inaccessible for any thiaporphyrin centered electrochemical process.

Negligible effects of the axial ligand on the mechanism and potentials of redox processes were observed except for the first reduction step of Cu(STpTP)X (Table 4). The latter process (eqn. (1)) involves the central metal ion, thus corresponding to the reduction of Cu(II) to Cu(I). A stabilization of the Cu(II) redox state of metallothiaporphyrin in the presence of Br^- and Cl^- as compared to ClO_4^- is

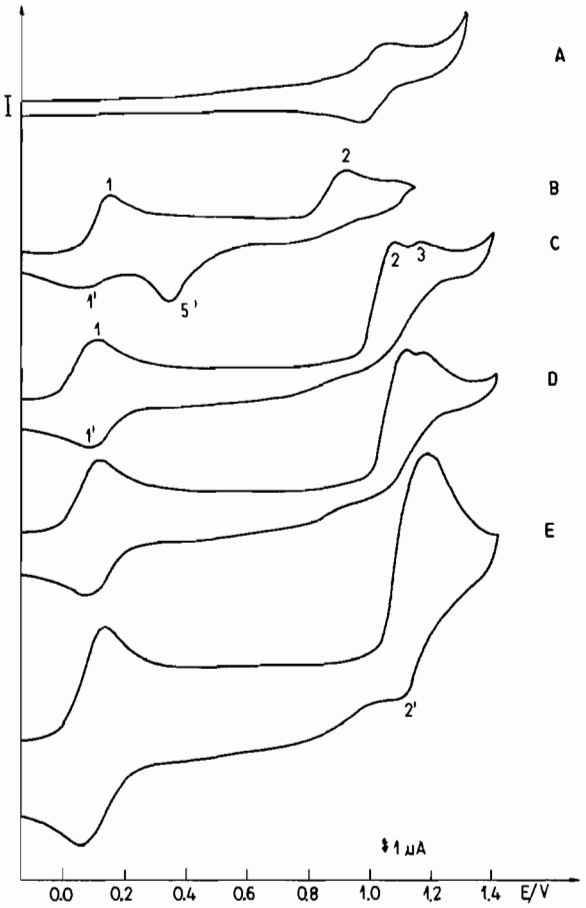

Fig. 5. Cyclic voltammograms of thiatetra(*p*-tolyl)porphyrin (STpTP) and its Cu(II) complexes. A, 1.3 mM STpTP in 0.1 M TABP–$C_2H_4Cl_2$, $\nu = 50$ mV s^{-1}; B, 0.7 mM Cu(STpTP)-HCO_3 in 0.1 M TBAP–CH_3CN, $\nu = 100$ mV s^{-1}; C, D, E, 1.3 mM $Cu(STpTP)HCO_3$ in 0.1 M TBAP–$C_2H_4Cl_2$, $\nu = 100$ mV s^{-1}, $\nu = 150$ mV s^{-1}, $\nu = 400$ mV s^{-1}, respectively.

TABLE 4. Characteristic potentials[a] determined from cyclic voltammograms for Cu(STpTP)X in 0.1 M TBAP–solvent at Pt electrode (temperature 298 K)

Solvent	X	2ox E_{pa}	1ox $E_{1/2}^r$	1red $E_{1/2}^r$ [b]	2–3red E_{pc}	2–3red $E_{1/2}$	4red $E_{1/2}^r$
$C_2H_4Cl_2$	HCO_3^-			+0.030[d]			
	HCO_3^-	+1.64	+1.20	−0.085	−1.10	−1.15[c]	−1.40
					−1.20		
	Br^-			−0.100			
	Cl^-			−0.130			
CH_3CN	HCO_3^-	+1.60	+1.17	−0.135	−0.92	−1.17[c]	−1.40
					−1.03		

[a] V vs. SCE, not corrected for the liquid junction potential. [b] 0.005 accuracy level; other values reported at 0.01 V. [c] Determined at $\nu = 500$ mV s^{-1}; other values determined at $\nu = 100$ mV s^{-1}. [d] One euqivalent of PPh_3 added.

observed and it follows the expected increase of the Cu(II) axial ligand bond strength. The addition of PPh_3 to the reaction medium makes the observed reduction process considerably easier, again in accord with the expected stabilization of the Cu(I) oxidation state by this ligand.

In a general case, when the reactant and the product of the electrode reduction will bind axial ligands, the following equation for the half wave potentials holds at 25 °C [39].

$$(E_{1/2})_c = (E_{1/2})_s - 0.059 \log(K_{Cu(II)}/K_{Cu(I)}) - 0.059 \log[L]^{p-q} \quad (11)$$

where $(E_{1/2})_c$ and $(E_{1/2})_s$ are the half wave potentials for complexed and uncomplexed species, respectively, $K_{Cu(n)}$ are the formation constants for copper (n) thiaporphyrin with ligands L, [L] is the free ligand concentration, q and p are the numbers of ligands axially bound to Cu(I)– and Cu(II)–thiaporphyrin, respectively.

Titration of $CuSTpTPHCO_3$–TBAP–$C_2H_4Cl_2$ by PPh_3 and Br^- added as TBABr has been performed and the half wave potentials for the Cu(II)/Cu(I) redox process determined as a function of the free ligand concentration. From the slope of the plot of $E_{1/2}$ versus log[PPh_3] or log[Br^-] the values $p-q$ (eqn. (11)) have been determined for the most typical systems studied. The complex dependence of $E_{1/2}$ and log[L] were observed for the entire concentration range investigated (the excess of the free ligand over the metallothiaporphyrin, n_L/n_{Cu}, ranged between 1 and 30) and the slopes have the opposite signs for both ligands, thus indicating quite a different preference for the complexation of Cu(II) and Cu(I) thiaporphyrins by these ligands. In the PPh_3 case the linear behaviour characterizes systems up to the free ligand concentration exceeding the concentration of the metallothiaporphyrin by a factor of 10 and the slope of the straight line is +0.066 V per decade. When the concentration of the free PPh_3 increases, the slope of $E_{1/2}$ versus log[L] curve decreases steadily.

The following scheme for the complexation is postulated to explain the observed behavior.

$$Cu(II)(STpTP)^+ + e \overset{PPh_3}{\rightleftharpoons} Cu(I)(STpTP)PPh_3 \quad (12)$$

$$Cu(II)(STpTP)PPh_3 + e \overset{PPh_3}{\rightleftharpoons} Cu(I)(STpTP)PPh_3 \quad (13)$$

A different characteristic is observed for the Br^- ligand. The linear behaviour is observed for the higher free ligand concentration investigated ($n_L/n_{Cu} > 15$) and its slope equals −0.053 V per decade, that gives $q = p - 1$.

At the lower concentrations the slope of the $E_{1/2}$ versus log [L] curve tends to zero. The above postulated changes in the stoichiometry of the complexes can also account for the Br^- behavior observed, i.e.

$$Cu(II)(STpTP)Br + e \rightleftharpoons Cu(I)(STpTP)Br^- \quad (14)$$

$$Cu(II)(STpTP)Br_2^- + e \overset{-Br^-}{\rightleftharpoons} Cu(I)(STpTP)Br^- \quad (15)$$

With an increase in the potential scan rates, considered waves overlap as a result of EC and CE processes at waves 2 and 3, respectively [40b]. At a higher potential scan rate the intermediate $[Cu(STpTP)]^{2-}$ can be detected on the anodic part of the cyclic voltammogram (wave 2′). A further support for the proposed mechanism can be found in the cyclic voltammogram for the reduction in CH_3CN (Fig. 5) where the reversible electrode processes of species generated by the chemical reaction can be noticed at a suitable time scale of the experiment (waves 3 and 3′). The half wave potential estimated for this electrode process is very similar to that determined for the first reduction of STpTPH. Wave 5′ appearing in the CH_3CN system corresponds to the oxidation of copper deposited on the platinum electrode and, as expected, its current increases with a decrease in the potential sweep rate. In 1,2-dichloroethane ratios of peak currents corresponding to successive reductions 1–3 (see Fig. 5) depend strongly on the concentration of Cu(STpTP)X. An enhancement of the current in the potential region of voltammetric waves 2–3 observed for these systems seems to be due to adsorption of electroactive species on the platinum electrode. The nature of the dependence of peak currents on the concentration of the electroactive material and on the potential scan rate indicate that the adsorbed species is mainly a product of the first electron addition to Cu(STpTP)X [40a]. However, the possibility of an electroactive reduction of 1,2-dichloroethane cannot be excluded [41]. The assignment of wave 5′ to the process

$$Cu(\text{on Pt}) \longrightarrow Cu(I)(CH_3CN)_n + e \quad (10)$$

was ascertained via independent cyclic voltammetry experiments performed for the reduction of $CuCl_2$ at Pt electrode in 0.1 M TBAP–CH_3CN. Peak potentials and shapes of the waves corresponding to the process (10) agree very well for both cases studied. The addition of the second electron to the Cu(II)(STpTP)X complex is followed by demetalation of metallothiaporphyrin. A similar decomposition was previously reported for the electrode reduction of other metalloporphyrins, i.e. PAg and PT1 (where P = TPP, $TPP(CN)_4$, OEP) [42, 43]. The second product of the decomposition is the thiaporphyrin anion $STpTP^-$, a strong base which can easily abstract proton from the reaction medium to give thiaporphyrin, STpTPH, that is reduced at the electrode to the corresponding anion radical. In both solvents a fourth redox couple can be seen on cyclic voltammograms for the reduction of 10^{-3} M Cu(STpTP)X solutions. The anodic–cathodic peak

separation and the peak currents characteristics indicate reversible electron transfer which was assigned to reaction (7). Voltammograms for the oxidation of Cu(STpTP)X complexes show anodic and two cathodic waves. Oxidation potentials are listed in Table 4 and suggest that successive abstraction of two electrons occurs at the thiaporphyrin ring system.

Conclusions

The replacement of one of the pyrrole rings of tetraphenylporphyrin by thiophene leads to an attractive modification of the molecule. The results concerning 21-thiatetra(*p*-tolyl)porphyrin and its copper complexes provide a novel example of metalloporphyrin and thiophene coordination chemistry.

The direct bond Cu–S(thiophene) is quite unique and its impact on the properties of the system under investigation unpredictable. The properties of STpTPH and its Cu(II) complexes are definitely different from those established for Cu(II) regular porphyrin, for instance Cu(II) thiaporphyrins exhibit a well defined Cu(II)/Cu(I) reduction reported previously only for Cu(II) N-substituted porphyrins.

It should be noted that straigthforward similarities do exist between the Cu(STpTP)X and Cu(NCH_3TTP)X systems. The Cu(NO–OEP) complex also presents similar features.

The modified equatorial donor (NCH_3; NO; S) imposes the decrease of the porphyrin cavity and deforms a planar TPP-like structure to a five coordinate geometry with the large out of plane displacement of the copper ion.

In our opinion the close structural resemblance of all structures causes the spectral and electrochemical similarities of these copper complexes with rather different tetraphenylporphyrin derivatives. The reduction of Cu(II) to Cu(I) can change the ionic radius of the central metal ion. The Cu(I) ion can be accommodated by both NCH_3TpTP^- and $STpTP^-$ as the Cu(II) ion is already displaced from the porphyrin plane. In the Cu(TPP) case the one electron reduction should be strongly cathodically shifted as the respective process requires severe geometry changes; this has not been described practically.

Generally porphyrin ligands stabilize high oxidation states of transition metal ions. The stability of high oxidation states can be related to the strong interaction and the ability of the porphyrin ligand to delocalize the positive charge via the conjugated system (π-donation). Decreased planarity diminishes the influence of these electronic factors and relatively destabilizes Cu(II) versus Cu(I) oxidation states. Relatively hard ligands, in the series studied, that bind well to Cu(II) (Cl^-, Br^-) give rise to the least favorable Cu(II)/Cu(I) potential shown. Additionally, it has the largest bathochromic shift of the electronic spectra and a similar hyperfine coupling constant A value. These results correlate well with the electronic and geometric structure changes influencing the electrochemical properties.

Acknowledgement

This work was supported by the Polish Academy of Science (Program CPBP 01.12 and 01.15).

References

1 D. Laneon, P. Cocolios, R. Guilard and K. M. Kadish, *J. Am. Chem. Soc., 106* (1984) 4472.
2 A. L. Balch, G. N. La Mar, L. Latos-Grazynski and M. W. Renner, *Inorg. Chem., 24* (1985) 2432.
3 A. L. Balch, Y. W. Chen, M. Olmstead and M. W. Renner, *J. Am. Chem. Soc., 107* (1985) 2393.
4 D. Mansuy, I. Morgenstern-Badaran, M. Lange and P. Gans, *Inorg. Chem., 21* (1982) 1427.
5 H. J. Callot, B. Chevrier and R. Weiss, *J. Am. Chem. Soc., 100* (1978) 1324.
6 S. Saito and H. A. Itano, *Proc. Natl. Acad. Sci. U.S.A., 78* (1981) 5508.
7 G. Augusto, K. L. Kunze and P. R. Oritz de Montellano, *J. Biol. Chem., 257* (1982) 6231.
8 L. Latos-Grazynski, R. J. Cheng, G. N. La Mar and A. N. Balch, *J. Am. Chem. Soc., 103* (1981) 4200.
9 B. Chevrier, R. Weiss, M. Lange, J. C. Chottard and D. Mansuy, *J. Am. Chem. Soc., 103* (1981) 2899.
10 L. Latos-Grazynski and A. Jezierski, *Inorg. Chim. Acta, 106* (1985) 13.
11 L. Latos-Grazynski, *Inorg. Chem., 24* (1985) 1104.
12 L. Latos-Grazynski, *Inorg. Chem., 24* (1985) 1681.
13 A. L. Balch, R. J. Cheng, G. N. La Mar and L. Latos-Grazynski, *Inorg. Chem., 24* (1985) 2657.
14 M. J. Bradhurst, R. Grigg and A. W. Johnson, *J. Chem. Soc. C,* (1971) 3681.
15 A. Ulman and J. Manassen, *J. Am. Chem. Soc., 93* (1975) 6540.
16 A. Ulman and J. Manassen, *J. Chem. Soc., Perkin Trans. I,* (1977) 1066.
17 A. Ulman, J. Manassen, F. Frolov and D. Rabinovich, *J. Am. Chem. Soc., 102* (1979) 7055.
18 A. Ulman, J. Manassen, F. Frolov and D. Rabinovich, *Inorg. Chem., 20* (1981) 1987.
19 L. Latos-Grazynski, J. Lisowski, M. M. Olmstead and A. L. Balch, *J. Am. Chem. Soc., 109* (1987) 4428.
20 D. A. Anderson, A. B. Kopelove and D. K. Lavalee, *Inorg. Chem., 19* (1980) 2101.
21 G. H. Barret, M. F. Hudson and K. M. Smith, *Tetrahedron Lett.,* (1973) 2887.
22 A. I. Vogel, in *Practical Organic Chemistry*, Wydawnictwa Naukowo-Techniczne, Warsaw, 1984.
23 H. O. House, E. Ferg and N. P. Peet, *J. Org. Chem., 36* (1971) 2374.
24 D. K. Lavallee and A. E. Gebala, *Inorg. Chem., 13* (1974) 2004.
25 A. Vohlberg and J. Manassen, *J. Am. Chem. Soc., 92* (1970) 2982.
26 E. B. Fleicher, *Acc. Chem. Res., 3* (1970) 105.
27 A. Stone and E. B. Fleischer, *J. Am. Chem. Soc., 90* (1968) 2735.
28 R. J. Abraham, G. E. Hawkes and K. M. Smith, *Tetrahedron Lett.,* (1974) 71.

29 J. J. Bonnet, S. S. Eaton, G. R. Eaton, R. H. Holm and J. A. Ibers, *J. Am. Chem. Soc., 95* (1973) 2141.
30 L. Latos-Grazynski and J. Lisowski, unpublished results.
31 B. J. Hathaway, *Struct. Bonding (Berlin), 37* (1984) 55.
32 (a) E. B. Fleischer, *J. Am. Chem. Soc., 85* (1963) 6667; (b) E. B. Fleischer, C. K. Miller and L. E. Webb, *J. Am. Chem. Soc., 86* (1964) 2342.
33 P. T. Manahoran and M. T. Rogers, in Te Wu Yen (ed.), *Electron Spin Resonance of Metal Complexes*, Plenum, New York, 1969, p. 143.
34 Y. Murakami, Y. Matsuda and K. Sakata, *Inorg. Chem., 10* (1971) 1734.
35 J. Subramanian, J. H. Fuhrhop, A. Salek and A. Gossauer, *J. Magn. Reson., 15* (1974) 19.
36 H. Yokoi, *Bull. Chem. Soc. Jpn., 47* (1974) 3073.
37 D. Kivelson and R. Neiman, *J. Chem. Phys., 35* (1961) 149.
38 P. W. Lau and W. C. Lin, *J. Inorg. Nucl. Chem., 37* (1975) 2389.
39 K. M. Kadish, in A. B. Lever and H. B. Gray (eds.), *Iron Porphyrins*, Part II, Addison-Wesley, Reading, MA, 1983.
40 (a) A. J. Bard and L. R. Feulkner, in *Electrochemical Methods, Fundamentals and Applications*, Wiley, New York, 1980, Ch. 12.5.4; (b) Ch. 11; (c) Ch. 5.
41 K. M. Kadish, X. Q. Lin and B. C. Man, *Inorg. Chem., 26* (1988) 4161.
42 K. M. Kadish, X. Q. Lin, J. Q. Ding and Y. T. Wu Araullo, *Inorg. Chem., 25* (1985) 3236.
43 A. Giraudean, A. Lourati, H. J. Callot and H. Gross, *Inorg. Chem., 20* (1981) 769.